NRL REPORT 3559

FR-3559

THE RIPPLE-TANK AS AN AID TO PHASE-FRONT VISUALIZATION

Allen H. Schooley

October 15, 1949

Approved by:

Dr. R. M. Page, Superintendent, Radio Division III

NAVAL RESEARCH LABORATORY

CAPTAIN F. R. FURTH, USN, DIRECTOR

WASHINGTON, D.C.

DISTRIBUTION

CNO	
Code 247	1
BuAer	
Attn: Code EL-51	1
BuOrd	
Attn: Re4f	1
ONR	
Attn: Code 470	1
Dir., SDC, ONR	
Attn: G. V. Amico	1
BuShips	
Attn: Code 833	1
Attn: Code 821	1
Attn: Jerome Spiegel-Electronics Div.	1
Dir., USNEL	
Attn: Code 300	1
Attn: Reports Unit	2
Attn: Dr. John B. Smyth	1
Dir., USNUSL	
Attn: Mr. C. M. Dunn	1
CO, NADS	
Attn: Dr. H. Krutter	1
Attn: Mr. E. Steele	1
Attn: Mr. E. R. Schlieben	1
CDR., USNOTS	
Attn: Reports Unit	2
BAGR, CD, Wright-Patterson AFB	
Attn: CADO-D1	1
Supt. USNPGS	
Attn: E. G. Goddard, Dept. of Electronics	1
CO, NATC	
Attn: Mr. L. S. Marquardt	1

CO, SCEL	
Attn: Dir. of Eng.	2
CO, USNPG - Dahlgren	1
OCSigO	
Attn: SIGGC-R-2	1
Attn: Mr. A. R. Beach	1
Attn: Ch. Eng. & Tech. Div., SIGTM-S	1
Dir., ESL	
Attn: Mr. O. C. Woodyard	1
Attn: Mr. Leonard Moore	1
CO, Headquarters, Strategic Air Command, Office, Air Base	
Attn: Electronics Section	1
Chief of Staff, USAF	
Attn: AFMEN-2	1
CG, AMC, Wright-Patterson AFB	
Attn: Major J. E. Lambert MCREEP	1
Attn: Mr. T. J. Gibbons MCREEO	1
Attn: Mr. R. E. Kester MCREER	1
Attn: Mr. A. L. Bell MCREER	1
Attn: George Rappaport MCREER	1
Attn: Eng. Div. Electronics Subdiv., MCREEO-2	1
CO, Cambridge Air Force Research Laboratories	
Attn: Dr. R. C. Spencer	1
Attn: Mr. R. M. Barrett	1
Attn: Mr. Walter Rotman	1
Attn: ERRS	1
CO, Watson Labs., AMC, Red Bank	
Attn: ENR	1
Office of Tech. Services, Dept. of Commerce	2
RDB	
Attn: Library	2
Attn: Navy Secretary	1
Attn: Committee on Electronics	1
Naval Res. Sec., Science Div. Library of Congress	
Attn: Mr. J. H. Heald	2

CONTENTS

ABSTRACT

The use of water ripples for the qualitative and semi-quantitative study of phase fronts near two-dimensional models of antenna structures deserves consideration by the electronics engineer. For this purpose, electronically driven probe-vibrators are used to excite the water surface of a glass ripple-tank. Synchronously chopped light is directed through the tank to a ground glass screen where the phase-front shadow patterns appear stationary. Using simple equipment, it is possible to visualize rapidly (or photograph) the changes in phase-front patterns brought about by changes in feed point position and in reflector configuration, as well as by changes of as much as several hundred percent in exciting frequency.

PROBLEM STATUS

This is a final report; exploratory research on the problem is concluded.

AUTHORIZATION

NRL Problem R99-01R

MOTION PICTURE FILM

In connection with this report there has been prepared a 10-minute, 16-mm silent motion picture film that shows ripple-tank demonstrations in which motion aids the process of visualization. Requests for the loan of this film should be addressed to the Technical Information Division, Naval Research Laboratory, Washington 25, D. C.

THE RIPPLE-TANK AS AN AID TO PHASE-FRONT VISUALIZATION

INTRODUCTION

In electronics work it is not unusual to have an antenna aperature across which the phase of radiation should be constant or vary in a particular manner. Often, in scanning systems, the beam tilt and the deviation from phase-front linearity with various placements of the feed point are of interest. Also it is desirable to know how the phase fronts are affected by changes in the excitation frequency. Since the calculation or experimental determination of phase-front patterns is usually a tedious operation, it appears that there is a need for a simple analog device to aid visualization of such patterns.

Since the ripple-tank is a device that has been used extensively to demonstrate most of the two-dimensional phenomena of physical optics,[1] it appeared suited for solving some problems of phase-front visualization met by electronics engineers. New techniques in the operation of the electronically driven ripple-tank were devised and applied to antenna problems, and photographs of phase-front shadow patterns near two-dimensional models of a few fimiliar antenna configurations were made.

EQUIPMENT

Basic components of the electronically driven ripple-tank are shown schematically in Figure 1. Audio oscillator (a) is used to drive synchronous motor (b) which has the slotted (light chopper) disk (c) attached to its rotor. The light from lamp (d) is projected through the slotted disk and through the glass ripple-tank (f) to the ground glass screen (e). Oscillator (a) also drives the electromechanical transducer (g) through impedance-matching device and attenuator (h). A probe attached to transducer (g) touches the surface of the water contained in tank (f) and excites ripples in synchronism with the pulses of light coming from lamp (d). Thus, the ripples, acting like cylindrical lenses, cast stationary light and shadow patterns upon the ground glass screen in accordance with the phase-front pattern set up in the ripple-tank. Mirror (i) is used for convenience in photographing the pattern by means of camera (j) or for eye-height viewing. Transducer (g) is shown in a track to provide for lateral movement. This movement, in connection with a motor drive (not shown), is of considerable help in setting up interesting demonstrations. For some experiments, more than one transducer is used.

Experimental equipment is shown in Figure 2. The audio oscillator (center) drives the light chopper (lower left) and also the transducers (left center). Above the transducers

---

[1] *Sutton, R. M., "Demonstration Experiments in Physics," pp. 149-154, New York: McGraw-Hill, 1938*

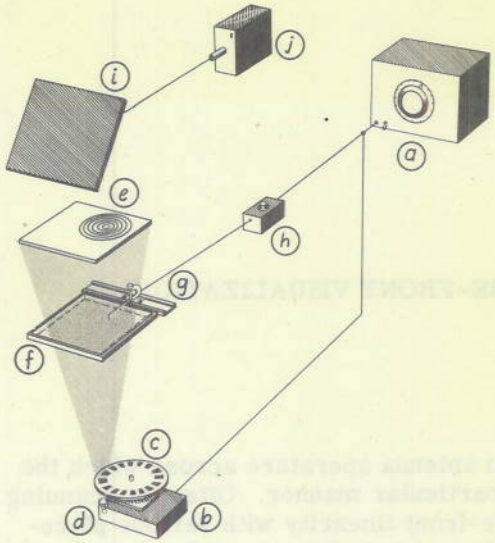

Figure 1 - Ripple-tank, schematic

is the ground glass screen, above the screen is the mirror tilted at a 45° angle and at the right a 16-mm motion picture camera is set up.

The 11-inch square ripple-tank shown in Figure 3 has beveled glass sides high enough to contain about 1/4-inch of water. Two electromechanical transducers are shown, one of which has a probe vibrator at the focus of a small parabola. The ground glass screen at the top of the apparatus is arranged so that its height can be varied.

The light, a 50 candle-power automobile headlight bulb, beneath the light chopper disk is shown in Figure 4. The disk is usually cut with the required number of slots to show one phase front for each cycle. However, for some demonstrations it may be advantageous to use one-half this number to spread out the pattern by showing every other phase front. On the other hand, twice the normal number of slots may be used to reduce the light flicker. In so doing the number of phase fronts in the pattern is doubled.

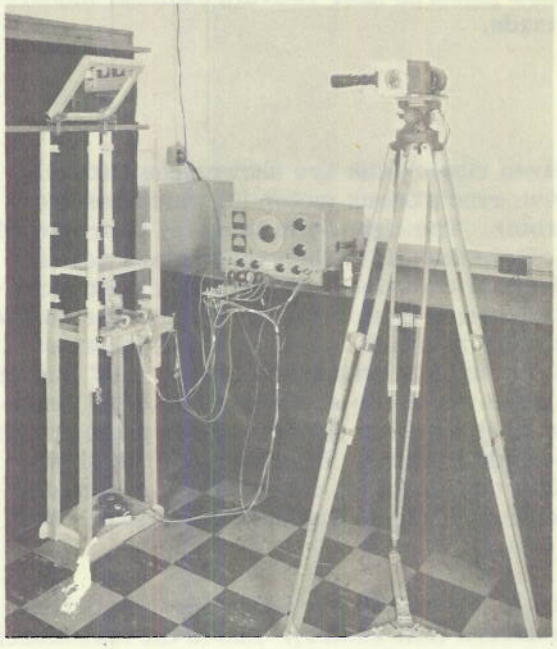

Figure 2 - Equipment

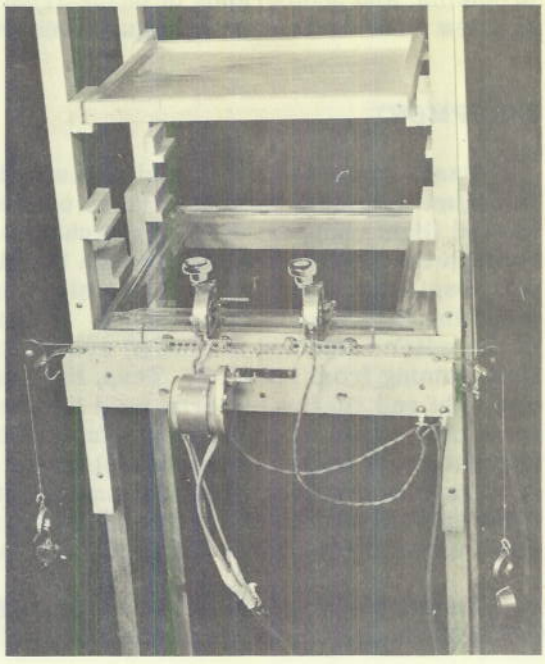

Figure 3 - Ripple-tank detail

PROPERTIES OF WATER RIPPLES AND RIPPLE-TANK TECHNIQUES

Intelligent use of the ripple-tank requires some knowledge of the techniques and limitations of ripple-tank operation. It is usually disturbing to note that the velocity of water-ripple propagation is dependent on wavelength, which is not the case for electromagnetic waves. The curve of Figure 5 shows theoretical ripple velocity (v) in cm per sec plotted versus wavelength (λ) in cm as calculated from the formula

$$v = (2\pi T/\lambda d + g\lambda/2\pi)^{1/2} \qquad (1)$$

where surface tension (T) is assumed to be the handbook value of 74.5 dynes per cm,

water density (d) is 1 gram per cm^3, and

acceleration of gravity (g) is 980 cm per sec^2.

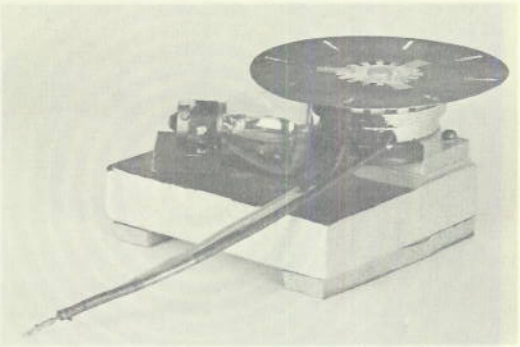

Figure 4 - Light and light chopper

Slightly below the theoretical curve are three points obtained experimentally by exciting the ripple-tank with a probe vibrating perpendicularly to the water surface first at 120, then 60 and, finally, 30 cycles per sec. In each case the wavelength was measured and the product of frequency and wavelength was used to determine the velocity. The discrepancy between the experimental points and the theoretical curve are explained by the slightly less than theoretical value of the water surface tension due to a small amount of contamination of the water by the soap used in cleaning the ripple-tank.

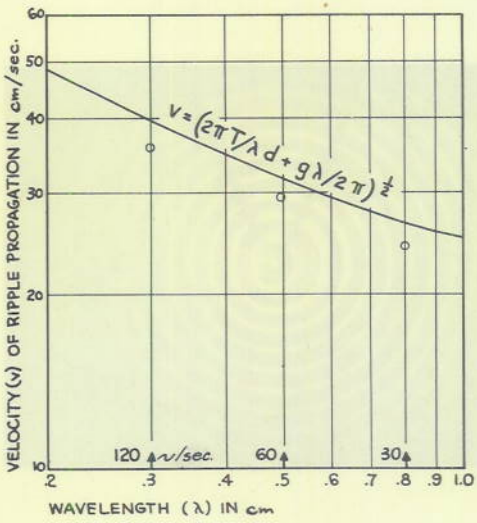

Figure 5 - Ripple velocity as a function of wavelength

Variation in velocity with wavelength is unimportant in most two-dimensional antenna model work because the basic scaling relationship that should be maintained is

$$d_m/\lambda_m = d_a/\lambda_a \qquad (2)$$

where d_m and d_a are corresponding dimensions of the model and antenna, respectively, and λ_m and λ_a are the wavelengths for the model and the antenna, respectively. Since most work requires the use of only one frequency at a time, it makes no difference what the velocity of propagation may be as long as the relationship in equation (2) is maintained. All measurements should be made in terms of wavelength and not in terms of frequency. It is interesting to note that the velocity of ripple propagation is less than the velocity of electromagnetic waves by a factor of the order of 10^9.

Figure 6 shows the shadow pattern of the phase fronts created by an isotropic source,

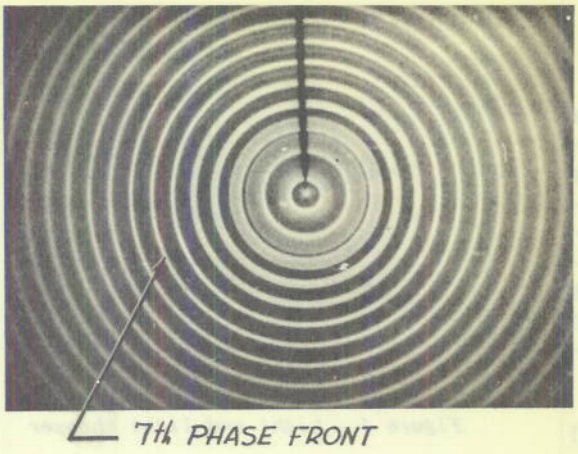

Figure 6 - Phase fronts from a point source

creating ripples of 0.24 cm wavelength when the light slots in the light chopper disk are about 6 percent of the opaque area. It is noticeable that the low-amplitude phase fronts near the edge of the picture are relatively faint and "fuzzy." Shadow patterns of the first two phase fronts overlap slightly. While the seventh phase-front pattern is relatively narrow and in relatively sharp focus. The phase-front shadows give a convenient method for measuring relative and absolute amplitudes of the waves. The crest-to-trough amplitude, A, of the narrow bright phase front, number seven, is approximately

$$A = 0.15\lambda^2(1/l_1 + 1/l_2) \quad (3)$$

where λ is the wavelength, l_1 is the distance between light-chopper disk and the water-surface and l_2 is the distance between water-surface and the ground-glass-screen. The crest-to-trough amplitude of the wide bright lines is given by the approximate expression

$$A = 0.15\lambda^2(1/l_1 + 1/l_2 + 3w/\lambda l_2) \quad (4)$$

where λ, l_1 and l_2 are the same as for equation (3), and w is the width of the bright shadow. The derivation of the above equations is given in the Appendix.

Using equation (3), the crest-to-trough amplitude of the seventh phase front was determined to be about 0.0008 inch; and using equation (4) the amplitude of the second phase front was found to be about 0.0028 inch. These and intermediate calculations show that the amplitude falls off as a linear function of the distance, within the experimental error, as would be expected for an isotropic exciter radiating in two dimensions.

The head of a pin which is vibrating perpendicularly to the water surface serves as the radiating probe in Figure 6. An adjustment of the transducer allows the edge of the pin head to be made even with the surface of the water. This minimizes the distortion of the phase-front patterns near the radiator due to a drawing up or depressing of the water surface. If such an adjustment is not made, the curvature at the water surface near the exciter may be large compared to the curvature of the ripples, and distortion of the pattern near the exciter will result. All phase-front pictures in this report are enlargements of single, 16-mm motion picture frames.

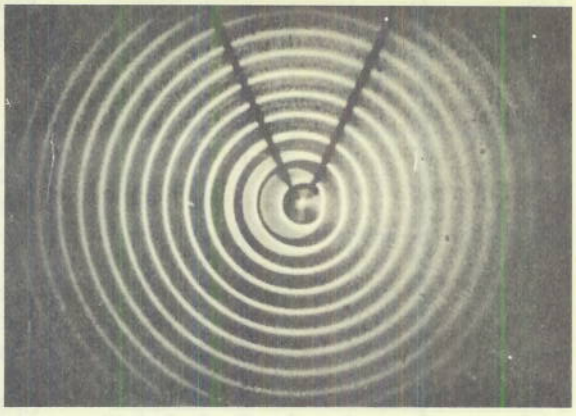

Figure 7 - Phase fronts from a point source with a small reflector nearby

Figure 7 is similar to Figure 6 except a round reflector, the diameter of which is small as compared with wavelength, is placed near the exciter to give some directivity to the pattern. This arrangement will be used as the primary feed pattern for several of the subsequent pictures.

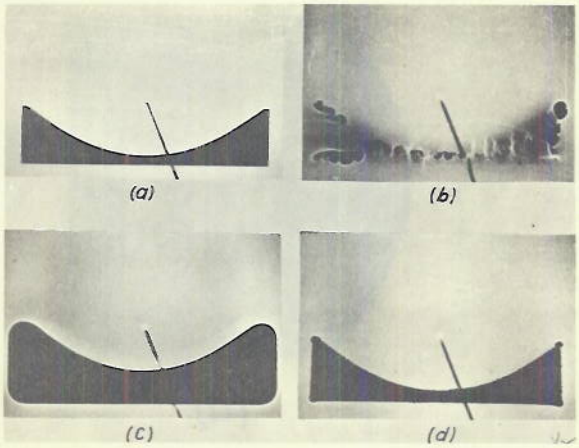

Figure 8 - Water contact angle distortion

Figure 8(a) shows the shadow pattern of an unexcited probe at the focus of a 1/4 in.-thick, 5 in.-aperature, brass parabola before water has been added to the ripple-tank, Figure 8(b) shows the same parabola when water has been added to a depth of about one-half the thickness of the parabola. It is seen that the irregular contact angle of the water with the side of the parabola distorts the water surface and this in turn distorts the shadow pattern to the point that the shape of the parabola is almost indistinguishable. Figure 8(c) shows the parabola shadow when the ripple-tank is filled higher than the level of the parabola but not sufficiently high to cover the top of the parabola. In this case the convex surface of the water near the parabola makes the shadow smooth, and larger than its actual dimensions. Figure 8(d) is the same parabola with the water level carefully adjusted with a syringe to just meet the sharp edge of the parabola at a contact angle as near 90 degrees as possible. Here the shape and size of the parabola is more nearly correct. The small irregularities are due to the fact that the edge of the parabola was not sufficiently clean and/or sharp. From the series of pictures in Figure 8 it is clear that care must be taken in preparing and using reflecting models in order to observe wave patterns near the reflecting surfaces without appreciable distortion.

In most demonstrations it is desirable to have a minimum of reflection from the sides of the ripple-tank. It can be shown that the amount of reflection from the edge of the tank can be greatly reduced if the water contact angle is made to approach zero. This is the condition of perfect wetting that holds for clean glass that has been scrubbed with soap and rinsed with water. Thus the edges of the ripple-tank should be made of glass and carefully cleaned before using. A beveled edge is of some additional help in reducing reflections.

RIPPLE-TANK PHASE-FRONT PATTERNS FOR A FEW ANTENNA CONFIGURATIONS

Figure 9(a) shows the phase fronts from a 1 1/4-centimeter "pillbox" antenna as reported by Iams[2] using a facsimile phase-front plotter for electromagnetic waves; and Figure 9(b) shows a ripple-tank, phase-front picture with about the same aperature to wavelength ratio. The two pictures are similar, although obviously not identical. In (b) the nonsymmetry of the pattern around the parabola axis indicates that the primary feed pattern was not as well directed along the axis as in (a). It is quite evident that some automatic gain control action was used in the equipment that produced (a), but no such

---

[2] *Iams, Harley, "Phase-Front Plotter for Centimeter Waves," RCA Review, VIII: pp. 270-275, June 1947*

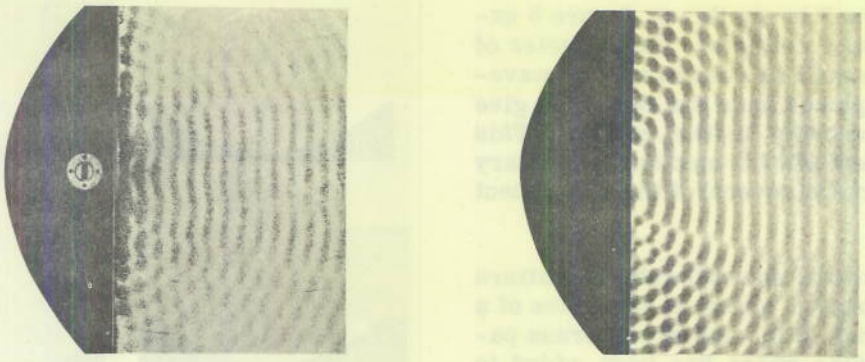

Figure 9 - Electromagnetic (left) and water ripple (right) phase fronts

action was possible in (b). The curved waves centered at the feed point, for both (a) and (b) make it apparent that the primary radiator in each case has appreciable back radiation. The irregularity of the center of the phase fronts near the feed point in each case indicates that the feed points are not precisely a whole number of 1/2 wavelengths away from the parabola. This will be demonstrated in the next figure.

Figure 10 shows the primary pattern of Figure 7 placed at the focus of a parabola. The wavelength was decreased for each successive picture. It is evident that the phase fronts in (a) and (c) are straighter than in (b) and (d) and the side lobes are less in the former than the latter. Although not immediately evidenced from the pictures, the feed point in (a) and (c) is 2-1/2 and 3 wavelengths, respectively, away from the parabola when measured along its axis—in (b) and (d) this distance is approximately 2-3/4 and 3-1/4 wavelengths, respectively. Thus, the ripple tank shows the desirability of having the focal length of the reflector a whole number of 1/2 wavelengths, when there is appreciable primary radiation in the direction of the secondary radiation. If a parabola of the proper focal length is not available it may be desirable to place the feed point as close to the focal point as is possible, consistent with the condition of having a whole number of 1/2 wavelengths between the feed point and the reflector.

Figure 11 shows the primary pattern of Figure 7 when placed at various points along the axis of a parabola. In (a) the concave-outward phase fronts indicate that the feed point is at less than the focal distance. In (b) the straight phase fronts indicate that it is at the focal point. In (c) and (d) the feed point is at successive distances greater than the focal lengths. All of the pictures in Figure 11 have a whole number of 1/2 wavelengths between the central point on the parabola and the feed point: these distances are 1-1/2, 2-1/2, 3 and 3-1/2 wavelengths, respectively.

Figures 12(a),(b), and (c) show a 12-wavelength aperture parabola fed by the primary pattern of Figure 7. In (a) the feed point is at the focus while in (b) and (c) the feed point is displaced at right angle to the axis through the focus by 10 percent and 14 percent of the aperture. The phase-front tilt for (a) is 0 degrees; for (b) about 14 degrees; and for (c) the phase front has deteriorated to such an extent that phase-tilt has lost its meaning. Figures 12(d), (e), and (f) show a circular reflector having the same aperture as above. In (d) the circle is fed at approximately the 1/2-radius point along the axis of the aperture and the phase-front tilt is 0 degrees. In (e) and (f) the feed point is displaced 10 percent

and 17 percent of the aperture giving resulting phase-front tilt angles of 13.3 and 27 degrees, respectively.

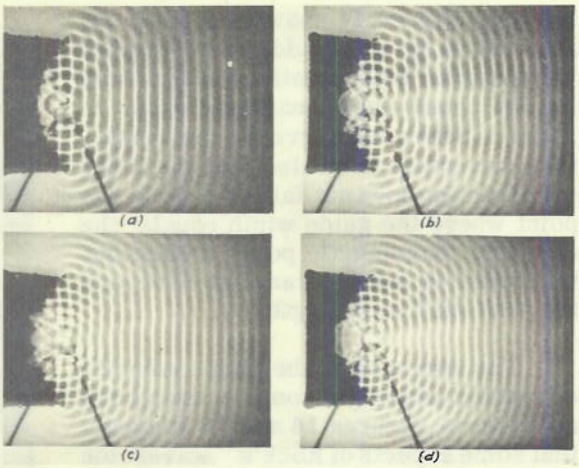

Figure 10 - Parabola fed at focus with frequency varied

Figure 13 shows a curve of phase-front tilt for various angles that a line connecting the feed point and the center of the reflector makes with the axis. The (x) points are for the parabolic reflector and extend no further than 14 degrees phase-front tilt because phase-front tilt beyond this point becomes meaningless. The (o) points show the circular reflector to give phase-front tilt angles that still have some meaning to more than 30 degrees. It is evident from Figures 12 and 13 that a circular reflector is more desirable than a parabola if considerable beam tilt is desired. In both cases the distance (F) between the feed point and the center of the reflector divided by the aperture diameter (D) was about 0.25. Beam deviation factor is defined as the ratio of feed-point off-set to phase-front tilt. This ratio for the straight line portion of Figure 13 is about 0.62. Van Atta and Keary[3] indicate that a microwave antenna having F/D = 0.25 will produce a beam deviation factor of about 0.73. Thus an error of about 15 percent is indicated.

Figure 14 shows a ripple-tank waveguide excited at the left end and transmitting energy to the right. The guide is formed by two closely spaced bars. In (a) the ratio of the wavelength outside the guide to the wavelength inside the guide gives a refractive index of 0.25. For (b) the exciting wavelength has been decreased by a factor of about 1.6 and the index is 0.46. From a series of similar pictures the curve shown in Figure 15 was obtained in which the index of refraction is plotted against the ratio of wavelength, λ, outside the guide to twice the guide spacing, b. The dashed quarter circle is the curve for a rectangular electromagnetic waveguide having negligible attenuation and operating in the TE_{01} mode. In this case the mode vanishes when the wavelength has been increased until it equals twice the waveguide width. The other curve was experimentally determined for the ripple-tank waveguide and it is evident that the two curves are far from quantitative agreement. It is interesting to

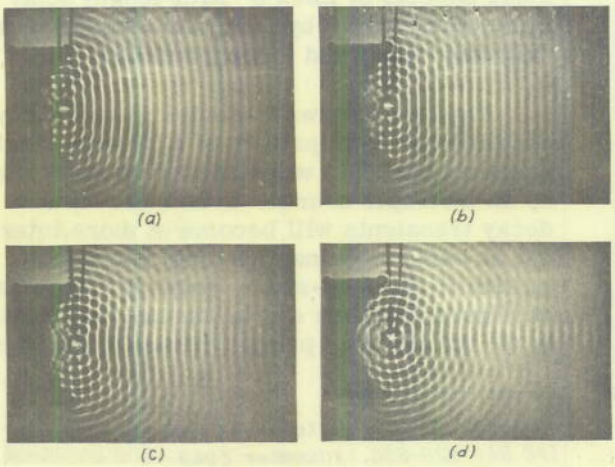

Figure 11 - Parabola-feed moved along axis

[3] *Van Atta, L. C., and Keary, T. J., "Shaped-Beam Antennas," Chapt. 13, pp. 465-509 in Silver, Samuel, "Microwave Antenna Theory and Design" Vol. 12, Radiation Lab. Series, New York: McGraw-Hill, 1949*

note that Figure 14 shows a substantial attenuation down the guide at the shorter wavelength. This situation does not hold for the usual electromagnetic case. In Figure 15 the solid curve for the ripple-tank waveguide indicates that the index of refraction does not fall to zero at the point where the guide width equals the one-half wavelength point, indicating that there is energy transmitted beyond the "cut-off" wavelength.

The increase in the phase velocity of ripples passing through a waveguide as shown in Figures 14 and 15 suggests that some aspects of Kock's[4] waveguide antenna may be simulated by the ripple-tank. Such a lens, shown in Figure 16, was designed for an index of refraction of about 0.55, and was made of 1/4-in.-thick brass, milled with 32 slots spaced 1/16 in. on centers. The slots were 0.040 in. wide and 3/32 in. deep; and the concave side had a radius of 1-1/4 in. Since there is no possibility of interference between the back radiation of the primary pattern and the secondary pattern in the case of the waveguide lens, the side lobe structure due to this cause

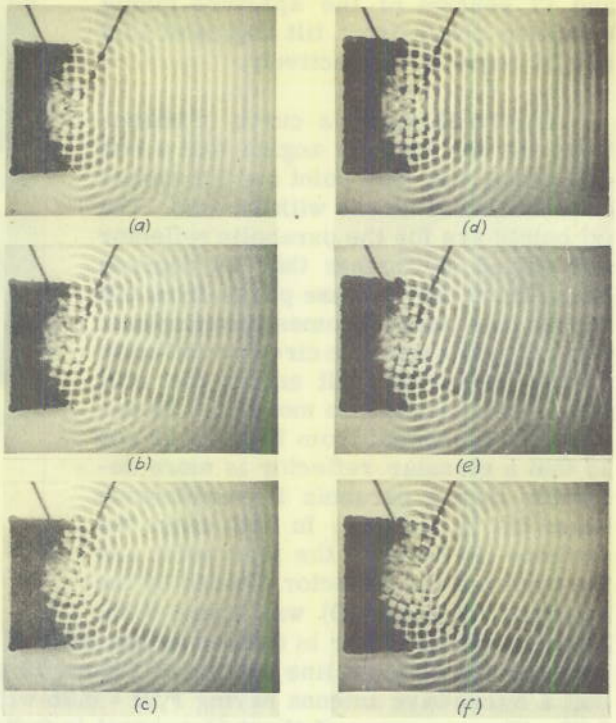

Figure 12 - Parbola (left) and circle (right) with feed point moved at right angles to axis

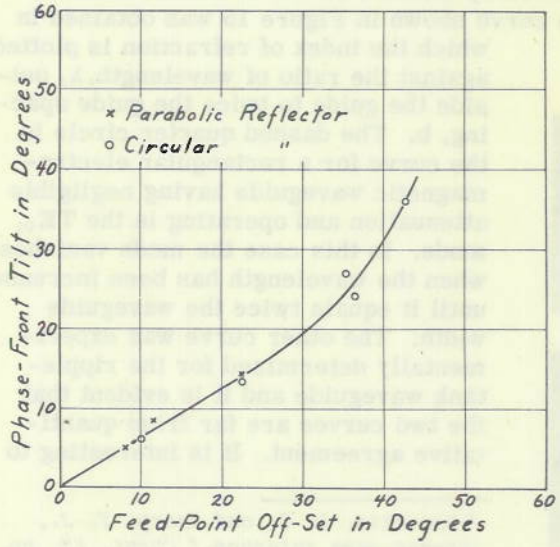

Figure 13 - Phase-front tilt vs feed-point off-set curve

is absent in Figure 16. Appreciable reflection from the first surface of the lens is evident. It should be possible to simulate some aspects of Kock's[5] path-length delay microwave lenses by using somewhat wider, "zig-zag" slots and a convex model.

Figure 17 shows the build up and decay of the phase-front pattern of a 24-wavelength aperture parabola when excited at the focus by an isotropic source. Such build-up and decay transients will become of more interest as radar antennas become comparable in size to the free-space length of the pulses. In Figure 17(a) the excitation has just started. In (b) the circular primary phase fronts have

---

[4] Kock, W. E., "Metal-Lens Antennas," Proc. IRE 34: 828-836, November 1949

[5] Kock, W. E., "Path-Length Microwave Lenses," Proc. IRE 37: 852-855, August 1949

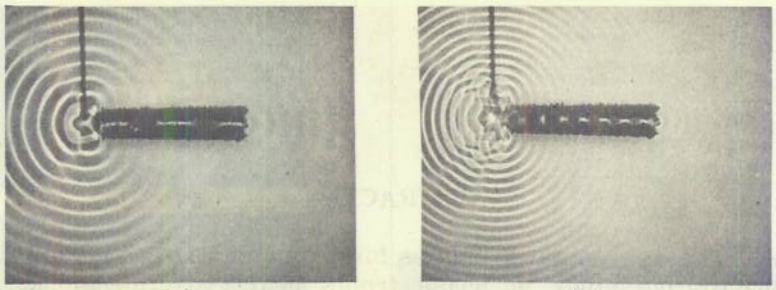

Figure 14 - A ripple-tank waveguide

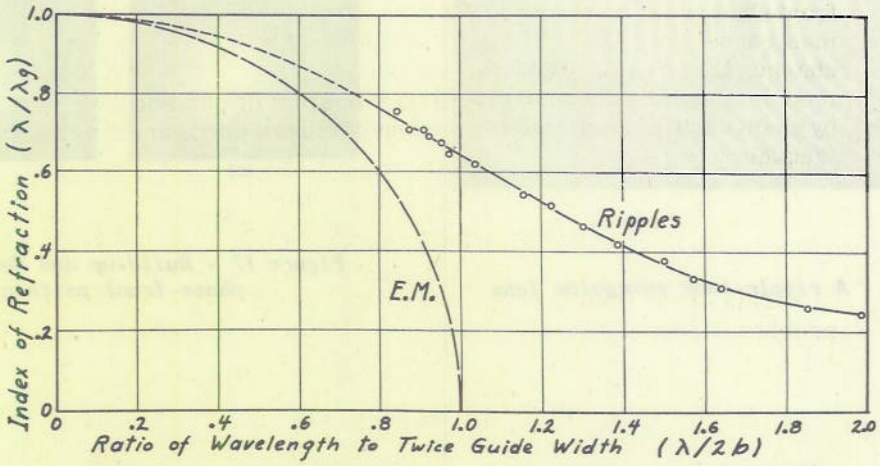

Figure 15 - Index of refraction curves for electromagnetic and ripple-tank waveguides

reached the edge of the picture while the straight reflected secondary phase fronts have almost reached the center. In (c) the steady state pattern created by the interference between the primary and secondary patterns is fully developed. The very poor steady state pattern is due to the isotropic primary source which is about the worst type one could select for feeding a parabola. In (d) it is evident that the primary radiation has been stopped but not for sufficient time to affect the secondary phase fronts. The secondary phase fronts are seen to be re-exciting the primary feed as they pass thus creating new low-amplitude, circular phase fronts. In (e) sufficient time has elapsed since the source has been shut off to allow the primary phase fronts to reach the edge of the picture while the last of the secondary phase fronts are approaching the center of the picture. Re-excitation of the primary feed is still evident. In (f) the straight secondary phase fronts have reached the upper part of the picture and all evidence of the severe side lobes of (c) has disappeared.

Figures 18(a), (b) and (c) show pictures similar to Figure 17 except in this case the water surface was pulse excited by water drops coming from an eye dropper. In (a) and (b) it is evident that the shorter wavelength components of the pulse travel faster than the longer wavelength components as would be expected from the curve of Figure 5. This

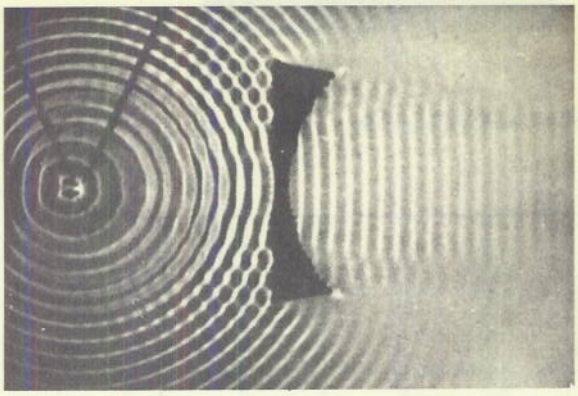

Figure 16 - A ripple-tank waveguide lens

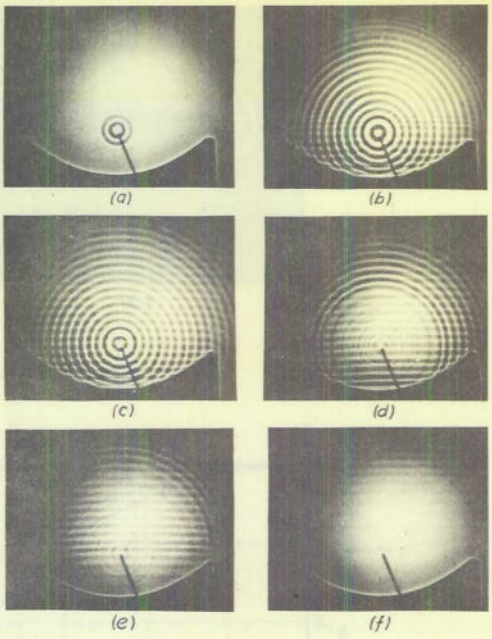

Figure 17 - Build-up and decay of a phase-front pattern

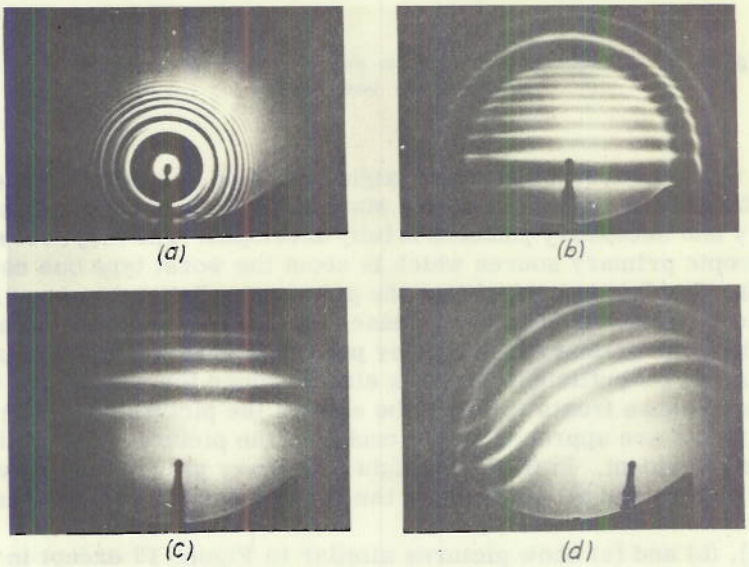

Figure 18 - Pulse excitation by means of water drops

phenomenon is of course absent in free space for electromagnetic waves. In (b) the time separation of the primary and secondary phase fronts is quite evident. In (c) the secondary pattern has progressed to the upper half of the picture. In (d) the parabola has been fed off axis and the tilt and curvature of the secondary phase fronts is quite evident. It is interesting to compare this with the steady state pattern of Figure 12(c). In Figure 18(d) the severe lobe structure is not evident as it is in Figure 12(c) because the primary and secondary phase fronts are time separated.

Figure 19 shows an aircraft silhouette receiving and reflecting the pulsed energy from a parabola with water drop pulse excitation as in Figure 18. In (a) the primary and secondary phase fronts are evident near the parabola. In (b) the phase fronts have reached the silhouette. In (c) the irregular phase fronts that have been scattered from the silhouette are evident. In (d) the reflected phase fronts are about to be received by the parabola. This demonstartion is not to the scale of any radar system because of several limitations to ripple-tank techniques.

Figure 20 shows pictures of phase-front and standing wave patterns near an aircraft silhouette for two different aspects. Phase-front patterns are shown in (a) and (b). Pictures (c) and (d) were taken under the same conditions as (a) and (b) except that the synchronous pulses of light have been replaced by a steady light. This was accomplished by

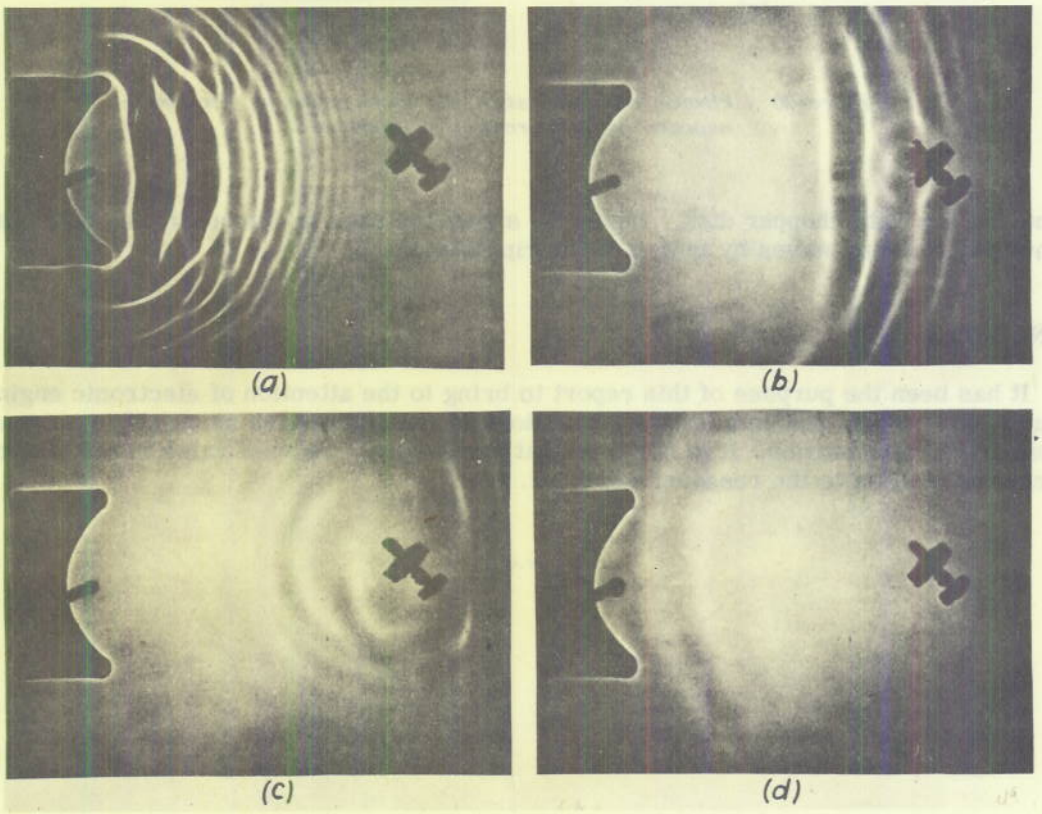

Figure 19 - Transmitted and reflected pulse

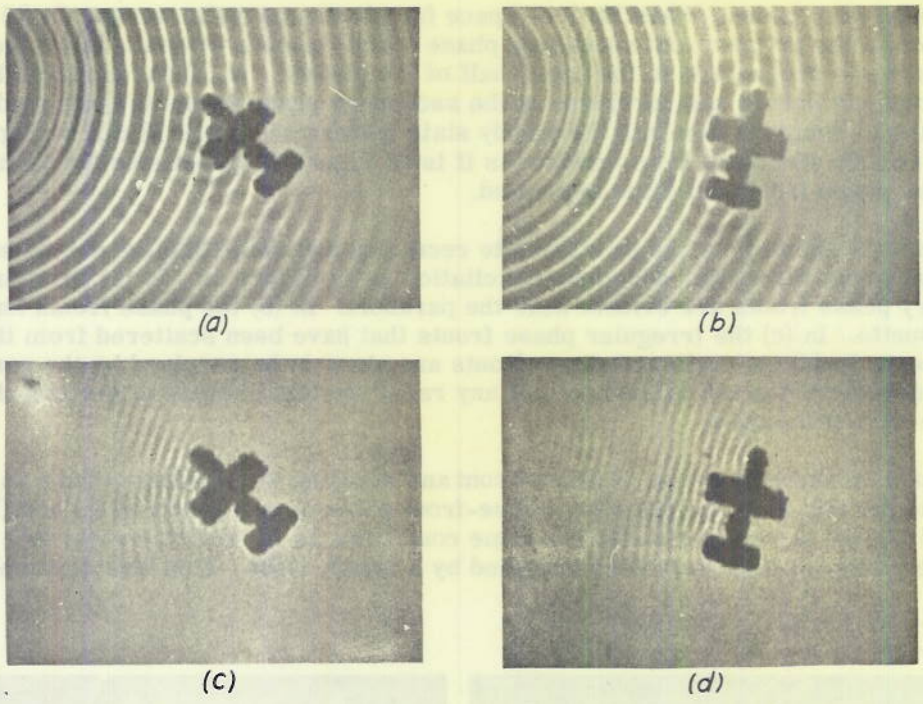

Figure 20 - Phase-front and standing wave patterns for two aspects of an aircraft silhouette

removing the light chopper disk. Figure 20 shows the ease in demonstrating both phase fronts and standing waves by means of the ripple-tank.

CONCLUSION

It has been the purpose of this report to bring to the attention of electronic engineers some of the virtues and some of the limitations of the ripple-tank as an aid to antenna phase-front visualization. It is believed that this device will be of value to the electronics teacher as well as to the research engineer.

* * *

APPENDIX
Derivation of Approximate Amplitude Expressions

For ripples of the wavelengths considered in this report the principal restoring force is the surface tension of the water. Under this condition it may be assumed that the shape of the ripples is sinusoidal. Figure 21 shows the refraction of parallel rays of light by one ripple having an index of refraction n = 1.33. In the ripple-tank the light source is over 200 wavelengths below the water surface and hence it is reasonable to assume parallel ray illumination. From the figure it is apparent that a ground glass screen placed near the top surface of the water will receive relatively uniform illumination. The slight bunching of the rays above the crest of the ripple will tend to make this region brighter than the regions on either side. As the ground glass screen is raised the bright region will become sharper until the focal point created by the top part of the crest is reached. By moving the ground glass screen beyond this point the image will widen. However the image will still remain quite sharp and bright as can be seen by the concentration of rays in the region above the focal point.

The above description explains the outer faint, fuzzy rings in Figure 6, as well as the intermediate narrow, bright rings and the wide, bright inner rings. In Figure 6, of course, the ground glass was held at a constant distance from the water while the focusing effects were produced by the linearly decreasing amplitude of the ripples with distance away from the source. A single intermediate ring does not appear as a very narrow bright line, as would be expected from the simple theory, because of the practical departure from a point source light and the finite width of the light chopper disk slots.

Figure 21 shows that the effective aperature of the crest-lens that produces focusing is about one-third wavelength ($\lambda/3$). The radius of curvature of the crest-lens is approximately equal to the radius of curvature of the sine wave at point (0). It can be shown that this radius of curvature is $r = \lambda^2/2\pi^2 A$ where A is the crest-to-trough amplitude of the sine wave. In Figure 22 the crest-lens is shown at the point marked "water"; and l_1, l_2, and l_3 are the distances to the light, to the ground glass, and to the focal point, respectively. From thin lens theory it is known that the radius of curvature, r, of a lens may be expressed as

$$r = \frac{n - 1}{1/l_1 + 1/l_3}$$

Substituting for r and n, it is possible to write

$$A = 0.15\lambda^2(1/l_1 + 1/l_3) \qquad (a)$$

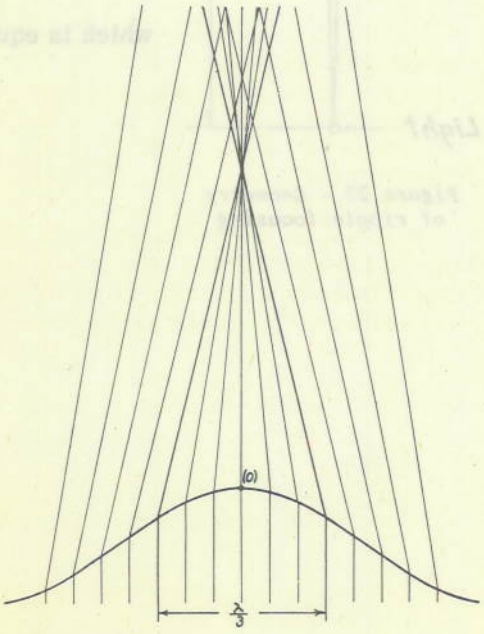

Figure 21 - Light refraction by a ripple crest

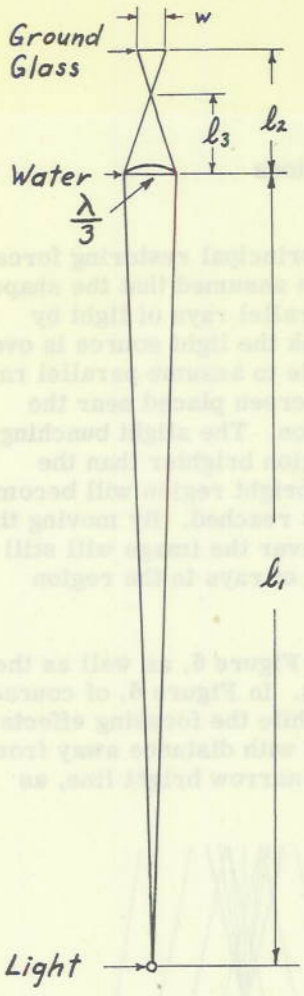

Figure 22 - Geometry of ripple focusing

which expresses the approximate crest-to-trough amplitude of the ripple in terms of wavelength, light-to-water distance, and water-to-focal-point distance.

From the geometrical arrangement in Figure 22, it is evident that the relationship between l_3 and w (the width of the bright region) is given by

$$\frac{w}{\lambda/3} = \frac{l_2 - l_3}{l_3}$$

or

$$l_3 = \frac{\lambda l_2}{\lambda + 3w}. \qquad \text{(b)}$$

Now, substituting equation (b) in equation (a) gives the crest-to-trough ripple amplitude in terms of the quantities usually measured. Thus

$$A = 0.15\,\lambda^2(1/l_1 + 1/l_2 + 3w/\lambda l_2) \qquad \text{(c)}$$

which is equation (4) of the text.

If the ground glass is placed at the focal point, w = 0 and the equation (c) becomes

$$A = 0.15\lambda^2(1/l_1 + 1/l_2) \qquad \text{(d)}$$

which is equation (3) of the text.

* * *